

Implantable probe with split anchors via residual stress and induced cell growth with gelatin nanofibres

Yu-Yen Chen¹, Bo-An Chen¹, Daniel Tsai¹, Cheng-Chun Huang¹, Jiasheng Yu², Wen-Pin Shih¹, Chii-Wann Lin³

¹Department of Mechanical Engineering, National Taiwan University, Taipei 10617, Taiwan

²Department of Chemical Engineering, National Taiwan University, Taipei 10617, Taiwan

³Institute of Biomedical Engineering, National Taiwan University, Taipei 10617, Taiwan

E-mail: wpshih@ntu.edu.tw

Published in *Micro & Nano Letters*; Received on 22nd July 2014; Revised on 24th October 2014; Accepted on 30th October 2014

A bipolar electrode probe used for implantable nerve stimulation treatments in minimally invasive surgeries is presented. The probe is composed of a flexible printed circuit substrate and a patterned SU-8 film. This probe features a three-dimensional (3D) tweezer-like mechanism opened by residual stress from the SU-8 film, designed to fix the probe in the tissue surrounding a target nerve. Stripes on the SU-8 film direct the net residual stress in a single direction to form a curve. The holding strengths of the probes with different deformations are defined and measured by a tensile test. Results show that the fixing ability of a 3D probe is better than a plane probe. The probes with curvature heights between 13 and 14 mm have a maximum average breaking force of 0.258 N, which is 16.3 and 13.1% higher than the probes with curvature heights between 9 and 10 mm and between 10 and 11 mm, respectively. In addition, a film of gelatin fibrous membrane, produced by electrospinning, covers the fixed ends of the probe's anchors and acts as cell scaffolds to induce cell growth, which help to ensure long-term fixation in the body. 3T3 fibroblast cells are grown to verify the scaffold effect of the fibrous membrane.

1. Introduction: Using electric signals, neural probes have been widely applied and used to record and to stimulate specific sites of the brain to combat various diseases. Some diseases can be relieved by pharmacological treatment, but long-term pharmacological treatments can cause many adverse side effects on the human body. Previous studies have shown that electrical stimulation on specific neural tissues can evoke different reactions [1]. The therapeutic effect of neural stimulation for pain relief is not permanent. From 1999 to 2004, clinical cases showed that the therapeutic effect lasts about 4–6 months on average [2]. To make treatments more permanent, implantable neural electrical stimulation systems have been developed to make the system more viable to treat various disorders, such as for Parkinson's disease [3] and sciatica [4, 5]. To address the invasiveness of implanting surgeries, minimally invasive surgery (MIS) procedures have been developed, which aim to reduce the size of incisions as well as a patient's discomfort after an operation [6].

A major issue of implantable stimulation systems is undesired movement from the stimulation probe. Human body movements will cause the probe to shift from its original place, making the therapy ineffective [7]. Thus, restricting the probe's movements is an important design consideration. In the opening surgery, keeping the probe fixed during the implantation process can be achieved in a variety of ways: with an anchor [8], with tissue adhesives [9], and with the surface structure design [10]. Both the surface structure and the anchor methods were implemented into the design of this probe to promote long-term fixation. Cell scaffolds with material and porosity are commonly investigated and widely applied to tissue engineering [11]. For MIS, a proper method to fix the probe is still lacking.

In this Letter, a bipolar porous probe with a tweezer-like split anchor and designed for MIS is presented. In the MIS, the probe will be implanted through a guiding needle, which has a diameter of 1.6 mm. The stable fixation of the probe is promoted initially by a tweezer-like split anchor and then by cells when they grow on the gelatin fibrous membrane. In this Letter, the stable fixation ability of the probe and the effect of the gelatin fibrous membrane will be demonstrated.

2. Probe design: The probe with a novel fixing method is developed by deforming a 2-dimensional (2D) plane probe with a 3D tweezer-like mechanism formed via the residual stress of the SU-8 film, allowing the probe to firmly clamp to the target nerve. Fig. 1 shows the probe structure. The probe is composed of a multi-layer flexible printed circuit (FPC) substrate, an SU-8 layer and a gelatin fibrous membrane. For smoothly passing into the guiding needle in MIS implantation, the width of the probe was restricted to less than 1.4 mm. Specifically, the probe is 30 mm long, 1.4 mm wide and 0.25 mm thick, as shown in Fig. 1.

The circuit design of the probe is shown in Fig. 1a. There are two connection pads that link the stimulation electrode pads at the back end of the probe to the stimulation system. The probe has two branches, and the widths of these branches are 0.6 and 0.8 mm, respectively. Two stimulation electrodes and an electric circuit are designed on the longer branch. The other branch is covered by the SU-8 film to deform the FPC and to form a tweezer-like split anchor. The curvature height was designed to be larger than the diameter of a target nerve, 5 mm, so that the split anchor can effectively accommodate the nerve. The fixing efficacy relies on the reaction exerted by the surrounding tissue on the split.

As shown in Fig. 1b, to improve long-term fixation, there are stripe structures on the SU-8 film to increase the surface roughness of the probe and to net the residual forces of the SU-8 film in a single direction for larger deformation. In addition, the gelatin fibrous membrane produced by electrospinning covers the fixed ends of the probe's bending branch and acts as a cell culture for cell growth to ensure long-term fixation in the body.

The probe is designed for long-term implantation, so the biocompatibility of the materials used was carefully considered. The FPC substrate is composed of polyimide and copper layers. Since copper is not an ideal material for implantation, gold was electrically plated above the part of the copper that may contact the tissue, to make the FPC substrate contain preferred materials for implantation [11]. The FPC flexibility was also desirable because it reduces damage caused by body motion [12]. SU-8 was adopted in the implantable medical device because of its biocompatibility and durability [13]. Gelatin was used because it is a natural

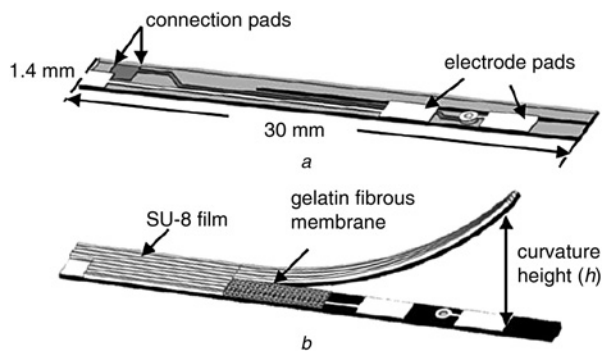


Figure 1 Probe design
a Basic circuit diagram of FPC probe containing a pair of electrode pads and two connection pads (one on top, one at bottom)
b Probe after addition of SU-8 film curves the FPC because of residual stress in SU-8 film

polymer with great biocompatibility and is widely applied in tissue engineering.

The fixing mechanism and implantable process of the probe is shown in Fig. 2. To clamp onto target nerve, the probe is inserted with the guiding needle. Once one end of the guiding needle reaches a location near the target nerve, the probe will be pushed out of the guiding needle, and then will clamp onto the nerve. Without the restraint of the needle wall, the split-anchor will open up because of the residual stress in the SU-8 film. Finally, the guiding needle will be taken out of the body so that the probe can be fixed and provide treatment by stimulating the target nerve.

3. Fabrication of the SU-8 film: The SU-8 film and the striped structure on the SU-8 film surface were defined by photolithography. The photolithographic fabrication process of the SU-8 film is shown in Fig. 3, and the parameters are listed in Table 1. The FPC substrate was attached on a glass wafer for fabrication. As the thickness of the SU-8 film should be greater than 100 μm to generate sufficient residual stress, SU-8 2150, which has high viscosity, was chosen. Hard contact was applied

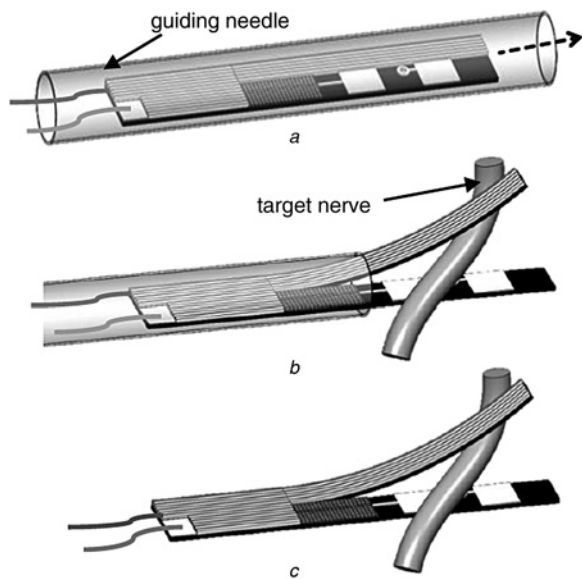


Figure 2 Process of implantation
a Inserting probe with guiding needle
b Pushing probe out of the guiding needle to accommodate the nerve
c Taking out the guiding needle from the body so that the probe can provide treatment by stimulating the target nerve

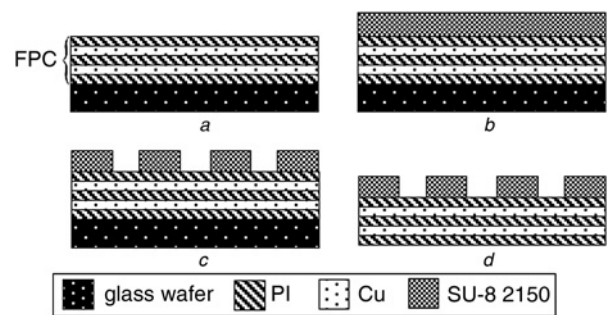


Figure 3 Fabrication process of the probe
a Attaching FPC on glass wafer
b Spin coating and exposing SU-8 on FPC
c Developing SU-8
d Removing FPC and SU-8 film from glass wafer

in the exposure step. After exposure, the sample was released from the glass wafer and hard baked to stabilise the SU-8 film.

After fabricating the SU-8 film, a laser was used to cut out the probe from the FPC. The final fabricated probe is shown in Fig. 4. The length of every stripe on the SU-8 film was 5 mm, and the distance between any two stripes was 1 mm, as shown in Fig. 4*a*. The probe curves because of the residual stress in the SU-8 film, as shown in Fig. 4*e*.

4. Fabrication of the gelatin fibrous membrane: The gelatin fibrous membrane was produced by the electrospinning technique [14]. For electrospinning of the gelatin fibrous membrane, 23% w/v gelatin/acetic acid (gelatin/AA) solution was prepared as the polymer solution. Particularly, gelatin of type-A from porcine skin in powdered form (Sigma-Aldrich) and AA solvent (Avantor) were chosen. To prepare the polymer solution, gelatin powder was soaked in AA for a day. Then, the powder was soaked in AA at 70°C for 5 h to completely dissolve the gelatin. After cooling down to room temperature, the solution was placed into a syringe (TEGUMO, 1 cc/ml). The electrospinning conditions for the gelatin/AA solution, which include the governing variables and environmental parameters, are shown in Table 2. For those fabrication parameters, the diameter of the electrospinning gelatin fibres ranged from 240 to 280 nm as shown in Fig. 5*a*.

Since gelatin has high water solubility, the electrospun gelatin fibrous membrane should be cross-linked before it is used as a cell scaffold. In our experiment, the gelatin fibres were cross-linked in glutaraldehyde vapour for a predetermined time at room temperature. The chosen concentration of glutaraldehyde was 50% (Sigma-Aldrich, 50% in H₂O). The cross-link time used was 1, 2 and 4 h, respectively. The morphology of the gelatin fibres was

Table 1 Process parameters to fabricate SU-8 film

Process	Parameters
coating (two steps)	(a) 500 rpm for 20 s (b) 3000 rpm for 60 s
soft bake (two steps)	(a) 65°C for 20 min (b) 95°C for 30 min
cooling	(a) 30 min
exposure	(a) 3600 μW/cm ² for 80 s
post-exposure bake (two steps)	(a) 65°C for 5 min (b) 95°C for 20 min
cooling	(a) 10 min
development	(a) 30 min
hard bake	(a) 150°C for 30 min

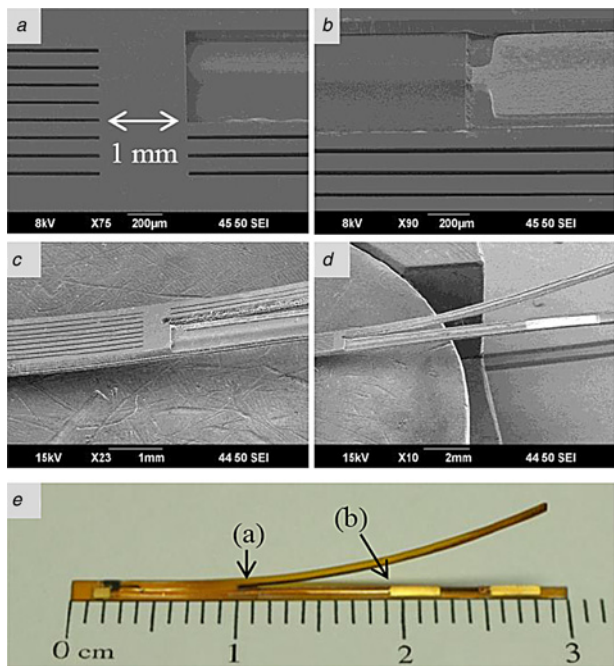


Figure 4 SEM photograph of probe and structure of SU-8, and photograph of probe
 a–d SEM photographs of probe and structure of SU-8
 e Photograph of probe

observed by a scanning electron microscope (SEM), as shown in Fig. 5. The results of this experiment show that the cross-link time affects the final diameter of the gelatin fibre and the pore size of the gelatin fibrous membrane. The diameter of the fibres increased with cross-link time while the pore size of the fibrous membrane decreased with increasing cross-link time. Since glutaraldehyde has cytotoxicity, cell activity and cell expansion could be affected by residual glutaraldehyde on the gelatin fibrous membrane [15]. Thus, after cross-linking, the gelatin fibrous membrane is thoroughly cleaned to remove residual glutaraldehyde on the membrane. The samples were then exposed in a fume hood under UV light for 4 days.

With increasing cross-link time, the residual glutaraldehyde on the membrane became more difficult to clean. The smaller pores hinder the cell from effectively growing into the membrane. Thus, the gelatin fibrous membranes cross-linked with glutaraldehyde for an hour was selected as the cell scaffold for this experiment because it had less residual glutaraldehyde and larger pores.

5. Residual stress in the film: In the probe design, the ratio of the thickness of the substrate to the SU-8 film is about 3:2, and the probe has a high aspect ratio of 21.43. Thus, the modified Stoney's formula is used to estimate the residual stress of the film

Table 2 Electrospinning conditions for gelatin/AA

Concentration	23% w/v
humidity	49%
temperature	25°C
rate	0.2 ml/h
voltage	15 kV
distance ^a	10 cm

^aDistance = distance between needle and collector

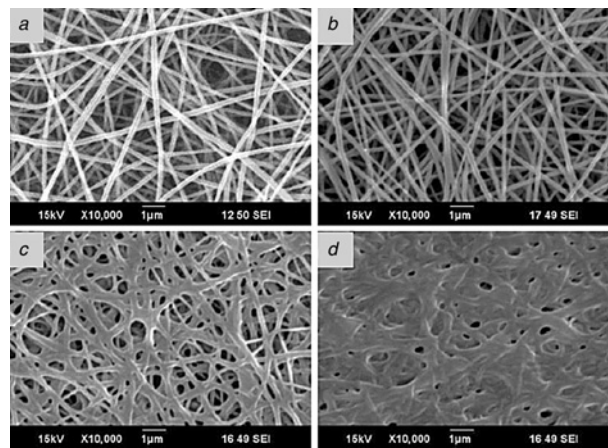


Figure 5 SEM pictures of electrospun gelatin fibres
 a Before cross-linking
 b–d After cross-linking with glutaraldehyde (50%) for 1, 2 and 4 h, respectively

[16]. The normalisation parameters used in Stoney's formula are

$$\delta = \frac{t_f}{t_s} \quad (1)$$

$$\gamma = \frac{E_f}{E_s} \quad (2)$$

$$\varphi = \frac{\bar{\sigma}_f}{E_f} \quad (3)$$

where t_f and $t_s = 148 \mu\text{m}$ is the thickness of the SU-8 film and the substrate, respectively. $E_f = 1.37 \text{ GPa}$ and $E_s = 4.7\text{--}5.2 \text{ GPa}$ is the Young's modulus of the FPC substrate and the SU-8 film thickness, respectively, and $\bar{\sigma}_f$ is the average residual stress in the SU-8 film.

The modified Stoney's formula is described as [16]

$$\rho = \frac{(1 + \gamma^3)\delta}{6\varphi\gamma(1 + \delta)} t_s \quad (4)$$

where ρ is the radius of the curvature of the substrate after deformation.

The thickness of the SU-8 film and the radius of the curvature were measured, and the residual stress of the films was obtained by applying the modified Stoney's formula. Fig. 6 shows the

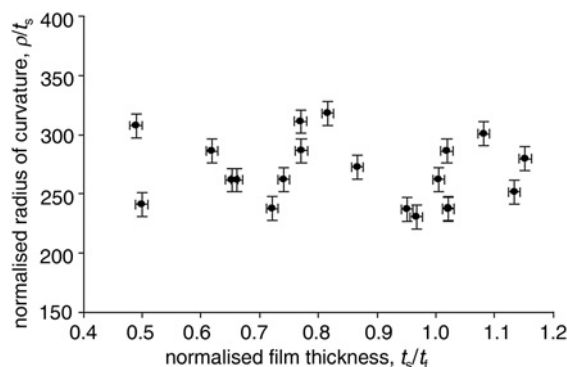


Figure 6 Relationship between film thickness and radius of curvature: graph of the SU-8 residual radius of curvature normalised by the FPC substrate thickness against the SU-8 thickness normalised by the FPC substrate thickness

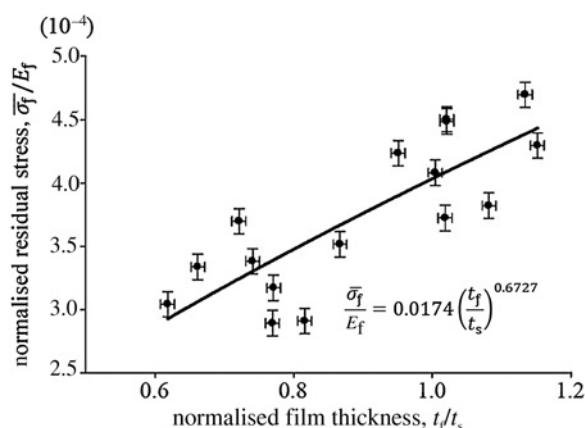


Figure 7 Relationship between the film thickness and the SU-8's residual stress: graph of the SU-8 residual stress normalised by its Young's modulus against the SU-8 thickness normalised by the FPC thickness

relationship between the film thickness and the radius of the curvature after the probe deforms. Fig. 7 shows the relationship between the thickness of the SU-8 film and the residual stress.

The results show no obvious relationship between the thickness of the film and the radius of the curvature, but a positive correlation between the residual stress of the SU-8 film and the thickness of the SU-8 film was obtained. Under the same fabrication condition, the residual stress in the SU-8 film was affected by the film thickness [17]. Owing to the non-uniform surface morphology of the FPC substrate, the thickness of the SU-8 film in this Letter ranged from 92.74 to 172.8 μm at a 3000 rpm spin rate on coating. In this range, thinner films were better than thicker ones because they had smaller residual stresses while maintaining similar radii of the curvature.

6. Cell culture: Initially, 3T3 fibroblast cells were seeded in a tissue culture polystyrene (TCPS) using a 96-well plate dish (cell density: 5×10^4 cells/cm²). A piece of electrospun gelatin fibrous membrane, cross-linked for 1 h, was then put into a well and fixed at the bottom of the TCPS by an O-ring. Cells were cultured in DMEM-HG medium (Thermo Scientific). The membrane was then left in the cell medium for 2 days. When the gelatin fibrous membrane was taken out, 3T3 fibroblast cells attaching onto the membrane were visible under an optical microscope (Olympus CKX41).

Fluorescence staining and scanning electron microscopy were used to ensure that healthy cells attached onto the membrane. After removing the original culture medium from each well, the sample was stained with 4',6-diamidino-2-phenylindole (DAPI) dye overnight at room temperature. Cell nuclei were stained by DAPI in blue. The morphology of the 3T3 fibroblast cells were stained with DAPI dye as shown in Fig. 8. The attachment of the 3T3 fibroblast on the membrane was confirmed through the merged image with the morphology of the 3T3 fibroblast cells and stained cell nuclei, as shown in Fig. 8c.

Different magnifications of SEM images of the 3T3 fibroblast cells are shown in Fig. 8. The structure of the gelatin fibrous membrane is complete and the 3T3 fibroblast cells grew very well. It was confirmed that cross-linking of gelatin for 1 h is sufficient to completely cross-link the gelatin fibrous membranes.

7. Tensile test: The holding strength, or the fixing capability, of the probe was evaluated by tensile tests. To test the holding strength of the probe in incision heals, 25% gelatin solution gel was used to simulate the muscle tissue because of the similar Young's modulus and the mechanical properties. The experimental setup and the tested specimen are shown in Fig. 9.

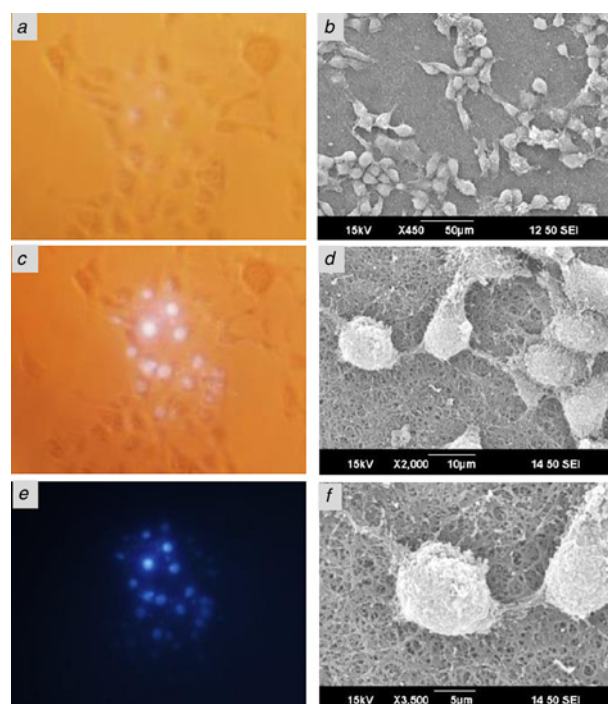


Figure 8 Morphology of 3T3 fibroblast cells (Fig. 8a); 3T3 fibroblast cell nuclei stained with DAPI dye in blue (Fig. 8b); merged picture of images of Figs. 8a and b (Fig. 8c); SEM images of 3T3 fibroblast cells under 450 \times (Fig. 8d), 2000 \times (Fig. 8e) and 3500 \times (Fig. 8f) magnification

Results from the tensile test are shown in Fig. 10. The horizontal axis denotes the normalised displacement, which is defined by the measured displacement divided by the probe length (D/L), of the load cell. The vertical axis denotes the measured tensile force from the load cell. In this test, the gelatin produced in different batches result in different Young's moduli and stiffness. Thus, to reduce the experimental error because of gelatin variations, the Young's modulus of the different batches of the gelatin should be measured and then used to normalise the tensile force. Specifically, the tensile force is normalised by the multiplication of the Young's modulus of gelatin and the total surface area of the probe. The point where the pulling force exceeds the adhesion force between the probe and gelatin is referred to as the break point. The tensile force at the break point is defined as the holding strength of the probe since it is the maximum force the probe can sustain.

The testing results in Fig. 10 indicate that the probes with curvature heights of 10.29 and 14.24 mm have the normalised holding strength of 0.24 and 0.26, which are 22.7 and 31.3% higher than that of the plane probe of 0.198, respectively. For the gelatin Young's modulus of 178.18 kPa and the probe total surface area of 85 mm², the normalised holding strength of 0.24 and 0.26 give the real holding strength of 0.368 and 0.398 N, respectively.

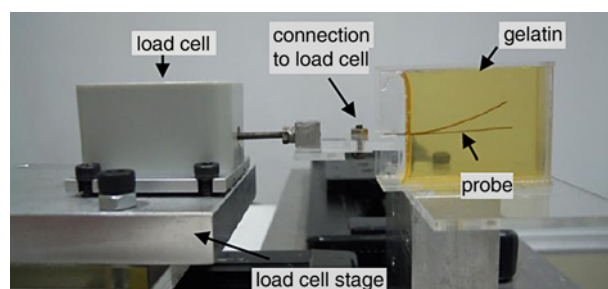


Figure 9 Experimental setup of the holding strength test: the probe specimen is inserted into the container before hardening the gel

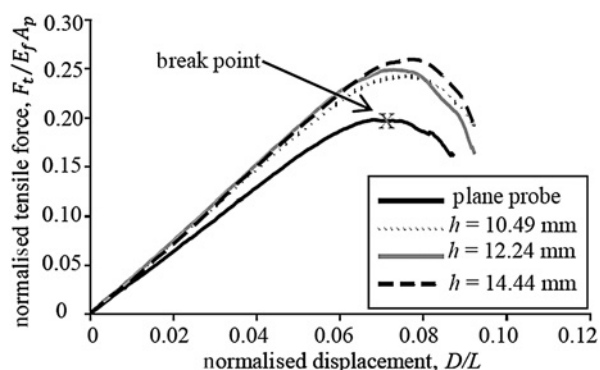


Figure 10 Tensile tests of probes bent by SU-8 in varying degrees and a control (without SU-8) Height (h) is shown in Fig. 1

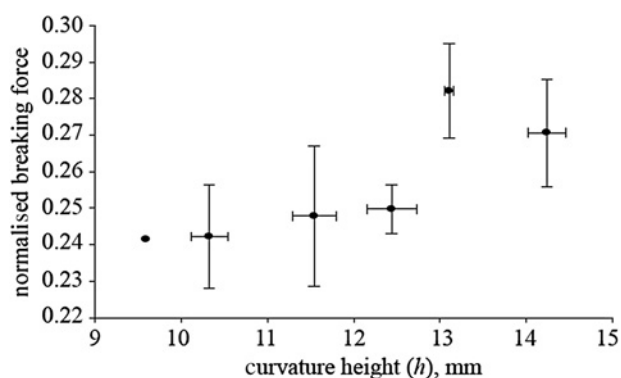


Figure 11 Relationship between average breaking force and curvature height: normalised breaking force against height

The relationship between curvature height and deformation of the probe is shown in Fig. 11. The normalised average holding strength of the curved probe with curvature heights between 13 and 14 mm is 0.258, which is 16.3 and 13.1% higher than those with curvature heights between 9 and 10 mm and between 10 and 11 mm, respectively. The average holding strength with a curvature height between 14 and 15 mm is 0.273, which is 4.4% lower than that between 13 and 14 mm. The fixing capability of the probe is optimal at a curvature height between 13 and 14 mm.

8. Conclusion: A 3D probe used for implantable nerve stimulation treatments in MIS implantation has been designed and tested. This probe featured a tweezer-like mechanism opened by the residual stress in the SU-8 film and a gelatin fibrous membrane for long-term fixation in the body.

The gelatin fibrous membrane, which is fixed on the probe, is proven to have good biocompatibility and mechanical properties for cell culturing. The cell scaffold attached onto the probe should reach the expected efficacy because the adhesion capability and growth of 3T3 fibroblast cells on the membrane are very ideal.

The holding strength test showed that the breaking force is determined by the probes with curvature heights between 13 and 14 mm,

which have a maximum average breaking force of 0.431 N. The thicknesses of the fabricated SU-8 films ranged from 92.74 to 172.8 μm , and the range of deformation of the probe ranged from 9 to 15 mm. A thinner film is preferable to a thicker one because it results in a smaller residual stress on the film while maintaining a similar curvature height.

9. Acknowledgment: This project was supported by the Ministry of Science and Technology, Taiwan, under the grant number: 103-2221-E-002-193-MY2.

10 References

- [1] Tehovnik E.J.: 'Electrical stimulation of neural tissue to evoke behavioral responses', *J. Neurosci. Methods*, 1996, **65**, pp. 1–17
- [2] Cahana A., Van Zundert J., Macrea L., Van Kleef M., Sluijter M.: 'Pulsed radiofrequency: current clinical and biological literature available', *Pain Med.*, 2006, **7**, pp. 411–423
- [3] Fuentes R., Petersson P., Siesser W.B., Caron M.G., Nicoletis M.A.: 'Spinal cord stimulation restores locomotion in animal models of Parkinson's disease', *Science*, 2009, **323**, pp. 1578–1582
- [4] Geurts J.W.M., Lou L., Gauci C.A., Newnham P., Van Wijk R.M.A.W.: 'Radiofrequency treatments in low back pain', *Pain Pract.*, 2002, **2**, pp. 226–234
- [5] Byrd D., Mackey S.: 'Pulsed radiofrequency for chronic pain', *Curr. Pain Headache Rep.*, 2008, **12**, pp. 37–41
- [6] Tendick F., Sastry S.S., Fearing R.S., Cohn M.: 'Applications of micromechatronics in minimally invasive surgery', *IEEE/ASME Trans. Mech.*, 1998, **3**, pp. 34–42
- [7] Shepherd R.K., Hatsushika S., Clark G.M.: 'Electrical stimulation of the auditory nerve: the effect of electrode position on neural excitation', *Hear. Res.*, 1993, **66**, pp. 108–120
- [8] Favre J., Taha J.M., Steel T., Burchiel K.J.: 'Anchoring of deep brain stimulation electrodes using a microplate: technical note', *J. Neurosurg.*, 1996, **85**, pp. 1181–1183
- [9] Bjarkam C.R., Jorgensen R.L., Jensen K.N., Sunde N.A., Sørensen J.C.H.: 'Deep brain stimulation electrode anchoring using BioGlue (R), a protective electrode covering, and a titanium microplate', *J. Neurosci. Methods*, 2008, **168**, pp. 151–155
- [10] Mahdavi A., Ferreira L., Sundback C., ET AL.: 'A biodegradable and biocompatible gecko-inspired tissue adhesive', *Proc. Natl. Acad. Sci. USA*, 2008, **105**, pp. 2307–2312
- [11] Karande T.S., Ong J.L., Agrawal C.M.: 'Diffusion in musculoskeletal tissue engineering scaffolds: design issues related to porosity, permeability, architecture, and nutrient mixing', *Ann. Biomed. Eng.*, 2004, **32**, pp. 1728–1743
- [12] Geddes L.A., Roeder R.: 'Criteria for the selection of materials for implanted electrodes', *Ann. Biomed. Eng.*, 2003, **31**, pp. 879–890
- [13] Zhong Y., Yu X., Gilbert R., Bellamkonda R.V.: 'Stabilizing electrode-host interfaces: a tissue engineering approach', *J. Rehabil. Res. Dev.*, 2001, **36**, pp. 627–932
- [14] Voskerician G., Shive M.S., Shawgo R.S., ET AL.: 'Biocompatibility and biofouling of MEMS drug delivery devices', *Biomaterials*, 2003, **24**, pp. 1959–1667
- [15] Deitzel J.M., Kleinmeyer J., Harris D., Beck Tan N.C.: 'The effect of processing variables on the morphology of electrospun nanofibers and textiles', *Polymer*, 2001, **42**, pp. 261–272
- [16] Wu S.C., Chang W.H., Dong G.C., Chen K.Y., Chen Y.S., Yao C.H.: 'Cell adhesion and proliferation enhancement by gelatin nanofiber scaffolds', *J. Bioact. Compat. Polym.*, 2011, **26**, pp. 565–577
- [17] Hui C.Y., Conway H.D., Lin Y.Y.: 'A reexamination of residual stresses in thin films and of the validity of Stoney's estimate', *J. Electron. Packag.*, 2000, **122**, pp. 267–273
- [18] Liu C.L., Tang D.P.: 'Effect of diamond film's thickness on thermal residual stress after considering the substrate's plasticity', *Adv. Mater. Res.*, 2011, **154**, pp. 1199–1202